

# Photometric and kinematic studies of open star clusters

## I. NGC 581 (M 103)

J. Sanner<sup>1</sup>, M. Geffert<sup>1</sup>, J. Brunzendorf<sup>2</sup>, and J. Schmoll<sup>3</sup>

<sup>1</sup> Sternwarte der Universität Bonn, Auf dem Hügel 71, D-53121 Bonn, Germany

<sup>2</sup> Thüringer Landessternwarte Tautenburg, Sternwarte 5, D-07778 Tautenburg, Germany

<sup>3</sup> Astrophysikalisches Institut Potsdam, An der Sternwarte 16, D-14482 Potsdam, Germany

Received 18 March 1999 / Accepted 12 July 1999

**Abstract.** We present CCD photometry and a proper motion study of the young open star cluster, NGC 581 (M 103). Fitting isochrones to the colour magnitude diagram, we found an age of  $16 \pm 4$  Myr and a distance of roughly 3 kpc for this cluster. The proper motion study identifies 77 stars of  $V = 14.5$  mag or brighter to be cluster members. We combine membership determination by proper motions and statistical field star subtraction to derive the IMF of the cluster and find a quite steep slope of  $\Gamma = -1.80$ .

**Key words:** Galaxy: open clusters and associations: individual: NGC 581 (M 103) – astrometry – stars: kinematics – stars: Hertzsprung–Russel (HR) and C–M diagrams – stars: luminosity function, mass function

### 1. Introduction

The shape of the initial mass function (IMF) is an important parameter to understand the fragmentation of molecular clouds and therefore the formation and development of stellar systems. Besides studies of the Solar neighbourhood (Salpeter 1955, Tsujimoto et al. 1997), work on star clusters plays an important role (Scalo 1986), as age, metallicity, and distance of all cluster stars can be assumed to be equal.

Most of the previous studies indicate that the IMF of a star cluster has the shape of power laws

$$N(m) \sim m^{\Gamma} \quad (1)$$

within different mass intervals. The following typical values of their exponents are given in Scalo (1998):

$$\begin{aligned} \Gamma &= -1.3 \text{ for } m > 10M_{\odot}, \\ \Gamma &= -1.7 \text{ for } 1M_{\odot} < m < 10M_{\odot}, \quad \text{and} \\ \Gamma &= -0.2 \text{ for } m < 1M_{\odot}. \end{aligned} \quad (2)$$

Knowledge of membership is essential to derive the IMF especially of open star clusters, where the contamination of the data

with field stars is a major problem. Two methods for membership determination are in use nowadays and each of them has its advantages and disadvantages:

- The classical method is to separate between cluster and field stars by their proper motions: All cluster stars can be expected to move in the same way, whereas the field stars show more widely spread and differently centred proper motions (see e.g. the recent work of Francic 1989). For each star a membership probability can be specified. To obtain a sufficient epoch difference, old as well as recent photographic plates are needed to measure proper motions, so that this method is limited by the comparably poor sensitivity of the old plates.
- With the introduction of CCD imaging to astronomy, statistical field star subtraction became more popular. Assuming (almost) identical field star distributions in the cluster region itself and the surrounding area, the distribution of the field stars can be subtracted from the one of the (contaminated) cluster area. This makes sense for fainter stars but with the bright stars one deals with statistics of small numbers.

Our work combines these two methods of membership determination: The proper motions are investigated for the bright stars of the cluster, whereas the fainter stars are treated with statistical field star subtraction. From the cleaned data we derive the luminosity and mass functions of the cluster.

NGC 581 (M 103), which is located at  $\alpha_{2000.0} = 1^{\text{h}}33.2^{\text{m}}$ ,  $\delta_{2000.0} = +60^{\circ}42'$ , was chosen as a first test object for our technique because the cluster *and* a sufficiently large field star region can be covered within the field of view of the telescope used. A  $V$  image of NGC 581 is shown in Fig. 1.

In Sect. 2 we present our CCD photometry, and in Sect. 3 a proper motion study of NGC 581 and another cluster which is located on the photographic plates, Trumpler 1. The resulting colour magnitude diagram (CMD) is discussed in Sect. 4, leading to the determination of the IMF of NGC 581 in Sect. 4.4.

### 2. CCD photometry

The photometry is based on 22 CCD frames taken in Johnson  $B$  and  $V$  filters at the 1m Cassegrain telescope of Hoher List

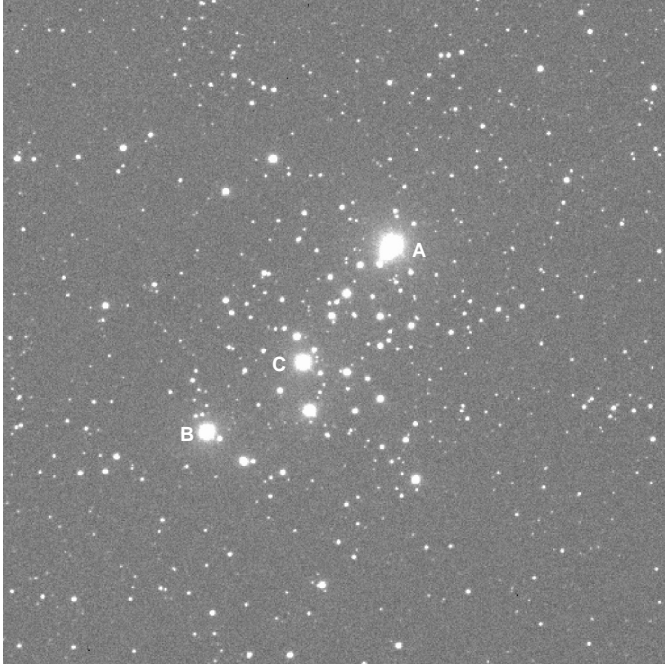


**Fig. 1.** 60 s  $V$  filter exposure of NGC 581 (M 103) taken with the 1m Cassegrain telescope of Hoher List Observatory. The field of view reproduced here is approx.  $15' \times 15'$ . North is up and east to the left. The stars marked as A, B, and C are mentioned in Sect. 4.2

Observatory. The telescope was equipped with a focal reducing system and a  $2k \times 2k$  CCD camera called HoLiCam (Sanner et al. 1998), which has a pixel size of  $15 \mu\text{m} \times 15 \mu\text{m}$  and a resolution of  $0.8''\text{pix}^{-1}$ . The field of view covered in this configuration is a circular area with a diameter of  $28'$ . Information about the images used for the photometry are summed up in Table 1.

The images of equal exposure times were averaged, resulting in integrated exposure times of 35 min in  $V$  and 60 min in  $B$  for the longest exposures. The shorter images were used to gain information about the bright stars which were saturated after longer exposure times. After standard image processing the photometry was performed with DAOPHOT II (Stetson 1991) running under IRAF. After an error selection process, the data were calibrated from instrumental to Johnson magnitudes using the photoelectric sequence of Hoag et al. (1961). Their standard stars as well as our instrumental magnitude values and their deviations are given in Table 2.

We applied the following equations to transform instrumental to apparent magnitudes:

$$v - V = a_0 - a_1 \cdot (B - V) \quad (3)$$

$$(b - v) - (B - V) = a'_0 - a'_1 \cdot (B - V) \quad (4)$$

with

$$a_0 = 5.536 \pm 0.04, \quad a_1 = 0.094 \pm 0.02 \quad (5)$$

$$a'_0 = 2.418 \pm 0.04, \quad a'_1 = 0.139 \pm 0.02 \quad (6)$$

where  $B$  and  $V$  represent apparent and  $b$  and  $v$  instrumental magnitudes, respectively. Mean photometric errors in different

**Table 1.** Summary of the CCD images from the 1m Cassegrain telescope at Hoher List Observatory used for the photometry and the proper motion study

filter	$t_{exp}$ [s]	number of exposures	
		photometry	proper motions
V	10	3	0
V	60	1	0
V	300	7	7
B	10	3	0
B	60	2	2
B	600	6	6

**Table 2.** Internal standard stars of Hoag et al. (1961) with the deviations of the computed from the catalogue magnitudes. Stars 1 and 2 were saturated even in the shortest exposures

no.	$V$ [mag]	$B - V$ [mag]	$\Delta V$ [mag]	$\Delta(B - V)$ [mag]
3	9.09	+0.21	-0.020	+0.039
4	10.45	+0.24	-0.038	+0.007
5	10.59	+0.17	-0.013	+0.002
6	10.81	+1.93	+0.004	-0.034
7	11.22	+0.23	-0.028	+0.015
8	11.35	+0.26	-0.002	+0.013
9	11.76	+0.22	-0.016	-0.022
10	11.84	+0.25	-0.031	+0.021
11	12.34	+0.10	+0.083	-0.105
12	12.76	+0.24	+0.090	-0.047
13	13.17	+0.30	-0.016	+0.023
14	13.21	+0.26	+0.012	-0.119
15	13.27	+0.44	+0.034	+0.019
16	13.46	+0.30	-0.009	+0.031
17	13.47	+0.35	-0.028	+0.075
18	13.59	+0.77	-0.001	+0.060
19	13.76	+0.30	-0.008	-0.010
standard deviations			0.036	0.051

**Table 3.** Photometric errors in different magnitude ranges

range	$\Delta V$ [mag]	$\Delta B$ [mag]
$V < 12 \text{ mag}$	0.007	0.009
$12 \text{ mag} < V < 16 \text{ mag}$	0.012	0.021
$16 \text{ mag} < V$	0.028	0.092

magnitude intervals are given in Table 3. One can see that the errors for  $B$  increase more rapidly as a consequence of HoLiCam's poorer sensitivity in blue wavelengths. Although the total exposure time in  $B$  was almost twice as large as in  $V$ , the limiting magnitude of the photometry is defined by the  $B$  images.

From these data, we determined a CMD which is shown in Fig. 2. It represents a total of 2134 stars for which both  $V$  and  $B$  magnitudes are available. We present the photometric data of all these objects in Table 4.

**Table 4.** List of the photometric data of all stars measured in the CCD field of NGC 581. Star numbers higher than 10,000 account for objects for which proper motions were determined, too. Only the ten brightest stars for which both photometry and proper motions are available are listed here, the complete table is available online at the CDS Strasbourg archive

No.	$x$	$y$	$V$ [mag]	$B - V$ [mag]
14380	1024.178	1122.116	10.603	0.168
14561	1136.343	1327.688	10.806	1.964
14503	1099.685	1056.475	11.028	0.177
14411	1046.961	1088.074	11.432	0.179
14288	972.818	1087.454	11.478	0.191
13899	697.822	446.703	11.674	0.530
13894	708.770	1589.465	11.776	1.917
14223	925.276	1073.279	11.776	0.242
14341	1003.143	1165.883	11.785	0.170
14928	1391.922	1103.418	11.871	0.229

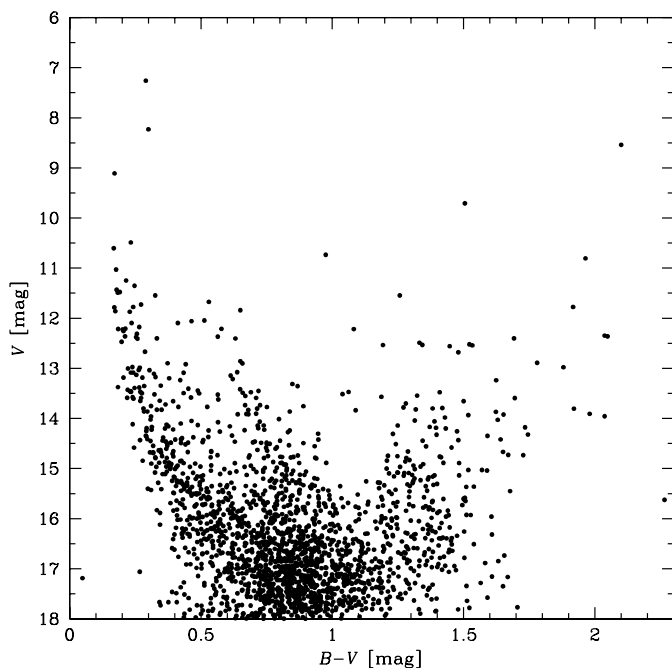


**Fig. 2.** Colour magnitude diagram of all objects detected on the CCD frames of NGC 581. Note the two main sequence structures and the scattered red giant branch. The origin of these features is discussed in Sect. 4

The CMD shows two main sequence features and a scattered giant branch in a colour range around  $B - V \simeq 1.4$  mag. More detailed analysis of the CMD is being presented in Sect. 4.

### 3. Proper motion study

#### 3.1. Data reduction

For the proper motion study eight photographic plates from the Bonn Doppelrefraktor (until 1965 located in Bonn, thereafter at Hoher List Observatory) were used, covering an epoch differ-

**Table 5.** Photographic plates from the Bonn Doppelrefraktor used for the proper motion study. The plates marked with MS were digitized with the PDS machines in Münster, the ones with T with TPS in Tautenburg. For comparison, both digitizations of R 0285 (Münster and Tautenburg) were used during data reduction

plate no.	date	$t_{exp}$ [min]	scan
R 0285	23.01.1917	30	MS/T
R 0294	09.02.1917	30	MS
R 0295	09.02.1917	3	T
R 1281	03.12.1977	60	MS
R 1291	05.12.1977	64	MS
R 1295	19.12.1977	4	T
R 1298	19.12.1977	4	T
R 1899	24.03.1998	60	T

ence of 81 years. The  $16\text{ cm} \times 16\text{ cm}$  plates of the  $D = 0.3\text{ m}$ ,  $f = 5.1\text{ m}$  instrument represent a region of  $1.6^\circ \times 1.6^\circ$ . The plates were digitized with the PDS machines of the Astronomisches Institut Münster and the Tautenburg Plate Scanner (TPS) of Thüringer Landessternwarte Tautenburg (Brunzendorf & Meusinger 1998). The positions gained with DAOPHOT II from 15 CCD frames were added to the plate data. Tables 1 and 5 give an overview of the material included in the proper motion study.

The celestial positions of the stars were determined from the plate coordinates with respect to six HIPPARCOS stars (ESA 1997) using an astrometric software package developed by Gefert et al. (1997). We obtained good results using quadratic polynomials (6 plate constants) for transforming  $(x, y)$  to  $(\alpha, \delta)$  for the photographic plates and cubic polynomials (10 constants) for the CCD images, respectively. The mean positional deviations of the HIPPARCOS stars after the first reduction step were of the order of  $0.1''$  in both right ascension and declination. Using the output positions and proper motions of each step as the basis of the next run, we derived a stable solution of proper motions of a total of 2,387 stars on the whole field after four iterations with a mean error for the proper motions of approx.  $1.1\text{ mas yr}^{-1}$  in both coordinates. The differences between our measurements and the HIPPARCOS data (“observed – calculated” or  $O - C$  values) are listed in Table 6. Compared with our measurements, HIPPARCOS star no. 7155 showed high deviations — probably caused by a double star nature of this object (Wielen et al. 1999) — and was therefore excluded before the data reduction. We present the proper motions of all stars in Table 7.

#### 3.2. NGC 581

228 stars were located within  $10'$  from the centre of NGC 581. Only these shown in Fig. 3 were taken into account for the vector point plot diagram. Due to the cluster’s large distance (see Sect. 4.2), the centres of the distributions of field and cluster stars are more or less the same. Therefore, the separation between field and cluster stars is not very apparent.

**Table 6.** "O – C" values of the measurements of the HIPPARCOS stars which were used for the transformation from pixel to celestial coordinates

star no.	$\Delta\alpha$ ["]	$\Delta\delta$ ["]	$\Delta\mu_\alpha \cos \delta$ [mas yr <sup>-1</sup> ]	$\Delta\mu_\delta$ [mas yr <sup>-1</sup> ]
6979	0.027	-0.020	0.22	-0.95
7640	-0.006	-0.080	-2.20	-1.38
7497	-0.006	-0.130	-0.91	-1.72
6793	-0.003	-0.020	1.17	2.40
6927	-0.011	-0.080	1.93	-1.10
6841	0.050	-0.330	-0.85	0.50

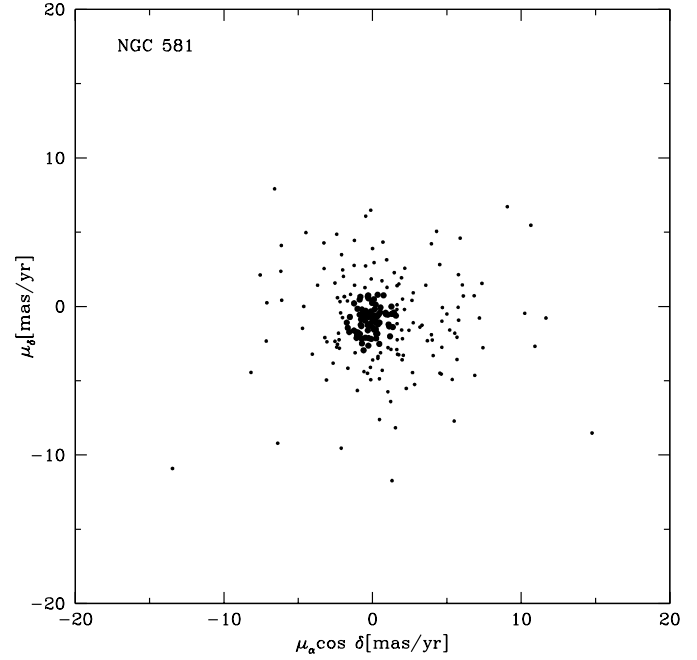
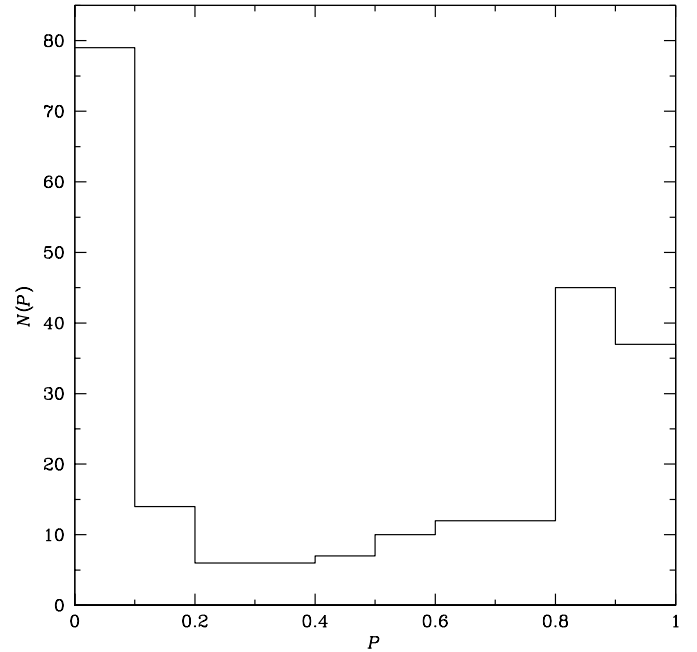
**Table 7.** List of all proper motions determined from the photographic plates of NGC 581. The positions are given for the epoch 1950.0 in the equinox 2000.0 coordinate system. The stellar numbers are the same as in Table 4. Only the proper motions of the same stars as in Table 4 are presented here, the complete table is available online at the CDS Strasbourg archive

No.	$\alpha$ [h m s]	$\delta$ [° ' "]	$\mu_\alpha \cos \delta$ [mas yr <sup>-1</sup> ]	$\mu_\delta$ [mas yr <sup>-1</sup> ]
14380	1 33 21.800	+60 40 12.25	-0.29	+0.74
14561	1 33 33.908	+60 42 59.62	-1.00	-1.74
14503	1 33 30.184	+60 39 19.62	-0.68	-0.53
14411	1 33 24.347	+60 39 44.88	+0.10	+2.95
14288	1 33 16.193	+60 39 43.50	-0.51	+1.27
13899	1 32 46.876	+60 31 02.94	+9.07	+6.72
13894	1 32 46.417	+60 46 26.62	+0.04	-1.44
14223	1 33 10.977	+60 39 31.50	+0.16	-0.18
14341	1 33 19.427	+60 40 47.50	-0.25	-1.30
14928	1 34 02.261	+60 40 00.25	-0.87	-0.55

According to the method presented by Sanders (1971), we fitted a sharp (for the members) and a wider spread (for the field stars) Gaussian distribution to the distribution of the stars in the vector point plot diagram. We computed the parameters of the two distributions with a maximum likelihood method. From the values of the distribution at the location of the stars in the diagram we derived the membership probabilities. Due to the small difference between the centres of the two distributions the stars with proper motions far away from the maximum are clearly identified as non-members, whereas it is difficult to decide which objects of the central region do belong to the cluster and which not. This is represented in the histogram for the membership probabilities (Fig. 4) with a clear peak at  $P \simeq 0$  and a much less pronounced increase towards  $P = 1$ . Fig. 5 shows the positions of the member and non-member stars.

With this method 77 stars were classified to be members of NGC 581 with a probability of at least 0.8, while 151 objects show a lower membership probability. The average proper motions for cluster stars are:

$$\begin{aligned}\mu_\alpha \cos \delta &= (0.11 \pm 1.07) \text{ mas yr}^{-1} \\ \mu_\delta &= (-0.95 \pm 1.24) \text{ mas yr}^{-1}\end{aligned}$$

**Fig. 3.** Vector point plot diagram of the stars in the region of NGC 581. Note that it is difficult to distinguish between the cluster proper motions and the centre of the field stars' proper motions. The stars with a membership probability of less than 0.8 are indicated by small, the others by larger dots. The width of the distribution of the stars with a high membership probability is of the order of 1 mas yr<sup>-1</sup> which coincides with the standard deviation of the proper motion of a single star**Fig. 4.** Histogram of the membership probabilities for the stars from Fig. 3

and for the field stars:

$$\mu_\alpha \cos \delta = (1.14 \pm 4.46) \text{ mas yr}^{-1}$$

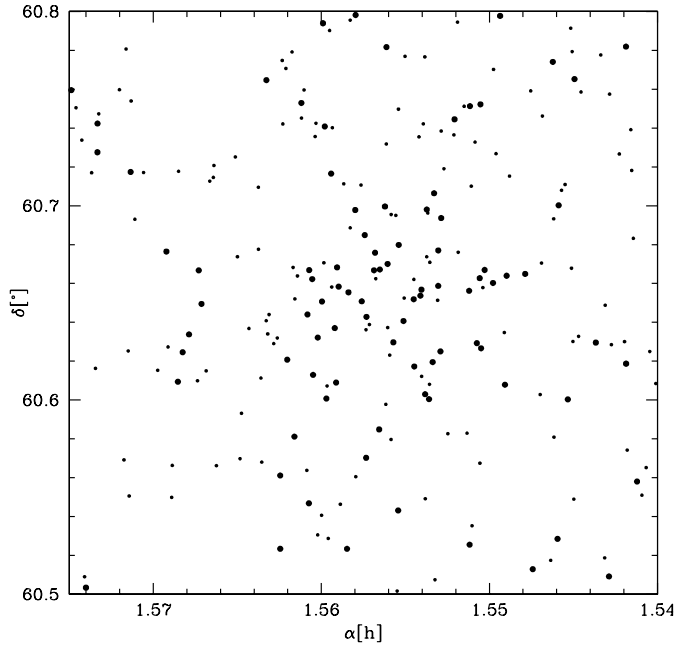


**Fig. 5.** Diagram of the  $(\alpha, \delta)$  positions of the cluster member and non-member stars due to the proper motions. The non-member stars are indicated by small, member stars by larger dots. Note that the field stars are distributed homogeneously over the whole area, however, the member stars are located in a larger than expected area. This point is discussed in Sect. 3.2

$$\mu_{\delta} = (-0.91 \pm 3.77) \text{ mas yr}^{-1}.$$

Although the values are very similar, the standard deviations show a large difference between field and cluster stars. We should remark that the “true” members might be more concentrated towards the cluster centre, but because of the problems in dividing between cluster and field stars, some non-members might be taken for member stars and vice versa.

### 3.3. Trumpler 1

Near the edge of the photographic plates we found the open star cluster Trumpler 1 for which we attempted a proper motion study, too, as a by-product of our work.

In a region of  $0.15^{\circ}$  around the centre of the cluster at  $\alpha_{2000} = 01^{\text{h}}35^{\text{m}}.7$ ,  $\delta_{2000} = +61^{\circ}17'$ , we detected only 64 stars on the base of the photographic plates. CCD photometry is not available. A membership analysis with the same methods as described above resulted in average proper motions of

$$\begin{aligned} \mu_{\alpha \cos \delta} &= (0.59 \pm 1.71) \text{ mas yr}^{-1} \\ \mu_{\delta} &= (-2.68 \pm 1.19) \text{ mas yr}^{-1} \end{aligned}$$

for the cluster members and

$$\begin{aligned} \mu_{\alpha \cos \delta} &= (1.41 \pm 5.73) \text{ mas yr}^{-1} \\ \mu_{\delta} &= (-4.59 \pm 3.93) \text{ mas yr}^{-1}. \end{aligned}$$

for the field stars. We present a vector point plot diagram in Fig. 6.

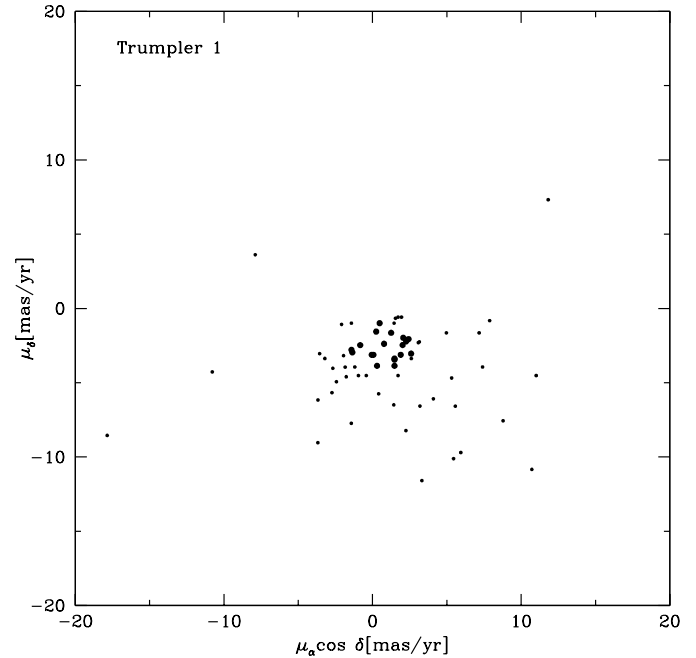


**Fig. 6.** Vector point plot diagram of the stars in the region of the open star cluster Trumpler 1. Again, the stars with a membership probability of less than 0.8 are indicated by small, the others by large dots. Be aware that this proper motion study is of less reliability than the previous one of NGC 581, as it is based only on photographic plates, and the cluster is located close to the edge of the plates

It should be mentioned that these proper motions are less accurate than our results for NGC 581, as Trumpler 1 is located close to the edge of the plates and we did not include CCD positions in our analysis. However, the results indicate that Trumpler 1 and NGC 581 have not only roughly the same ages and distances (see Phelps & Janes 1993), but — within the errors — the same absolute proper motions. Therefore, the two objects may be taken as a candidate for a binary star cluster (see e.g. Subramaniam et al. 1995) as they are known for the Magellanic Clouds (Dieball & Grebel 1998).

## 4. Analysis of the colour magnitude diagram

### 4.1. Field star subtraction

The CMD derived in Sect. 2 is contaminated with field stars. Before trying to analyse the CMD it is essential to subtract these stars to emphasise the features which belong to NGC 581 and to prepare the data for the determination of the cluster IMF.

In the magnitude range covered by the proper motion study it is possible to distinguish between field and cluster stars using the information of the membership probabilities from Sect. 3. The proper motion study is complete down to  $V = 14$  mag so that until this point, a membership probability of 0.8 or higher is considered a suitable criterion for the definition of the members of NGC 581.

Below this limit, the star numbers are high enough to justify a statistical field star subtraction. For this, the CCD field was

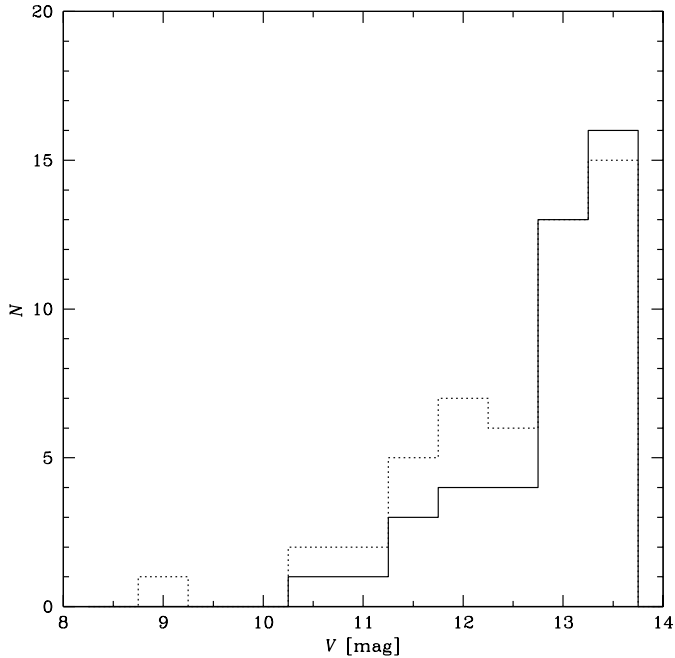


**Fig. 7.** Luminosity functions down to  $V = 14$  mag according to field star subtraction with proper motions (solid line) and statistical subtraction (dotted line). Statistical field star subtraction for the brighter stars would have led to 9 additional cluster members and therefore to a shallower IMF

divided into two regions of the same area of  $1.3 \cdot 10^6$  pixels: a circular region with the star cluster in its centre (radius: 654 pix. or  $18'$ ) and a ring encircling this region (outer radius: 925 pix. or  $26'$ ). Under these assumptions, all cluster members are surely located in the central area. For both parts separate CMDs were computed. Each of them was divided into rectangular bins with a length of 0.5 mag in magnitude and 0.1 mag in colour. (Variation of the bin sizes did not affect the results.) The numbers of stars in the field CMD cells were determined and as many stars of the corresponding cell of the inner region CMD were randomly chosen and removed. Assuming a homogeneous distribution of field stars over the whole field of view, the resulting CMD, which is presented in Fig. 8, represents only the cluster members.

To illustrate the advantage of our method, Fig. 7 shows the luminosity functions obtained with the proper motions and the statistical field star subtraction, respectively, in the range of the photographic plates ( $V < 14$  mag). It can be seen that the proper motion analysis leads to less member stars than the statistical subtraction.

#### 4.2. Morphology of the cluster CMD and age determination

The brightest stars in the field of NGC 581 (marked with letters A to C in Fig. 1) were saturated even in the shortest exposures so that no direct photometric information was available for them. However, the three stars were the subject of previous photoelectric studies (Hoag et al. 1961, Purgathofer 1964) so that their  $V$  magnitudes and  $B - V$  colours could be added to our CMD manually. Star A was too bright to be measured on the photographic

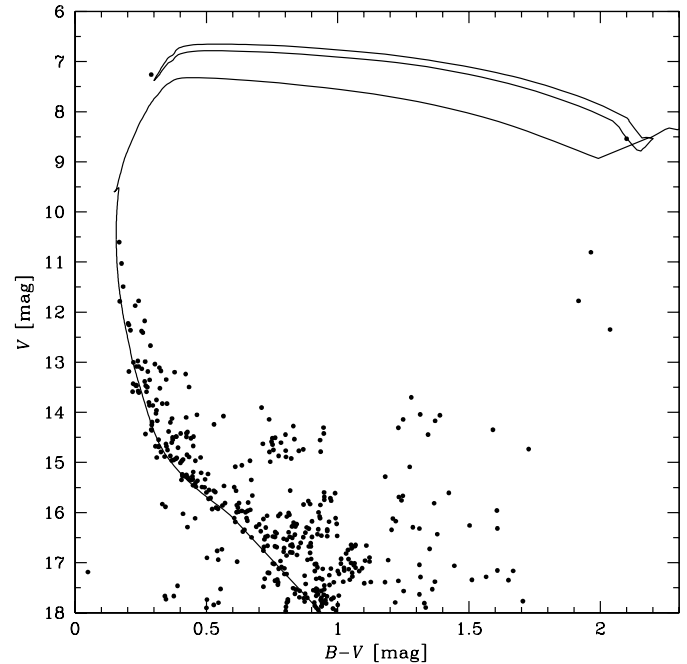


**Fig. 8.** Colour magnitude diagram of all members of NGC 581 as determined with the proper motions ( $V < 14$  mag) and the statistical field star subtraction ( $V > 14$  mag). The parameters of the isochrone plotted in the diagram are listed in Table 8. Note that the brightest star of Fig. 2 is not a member of the cluster

plates with a sufficient accuracy so that we could not derive its proper motion, either. However, since star A is a HIPPARCOS star (ESA 1997, star no. 7232), we could get its proper motion from this source. Calculating its membership probability led to a value of 0.89. Star B has a proper motion far away from the one of the cluster so that it can be considered a non-member, while star C belongs to NGC 581 with a probability of 0.90.

After field star subtraction, we found three red stars with  $B - V \approx 2$  mag from  $V \approx 10.8$  mag to  $V \approx 12.4$  mag. Compared with the well populated main sequence in the same magnitude range, it seems obvious that these objects cannot be cluster members. We assume these objects to be field stars which are classified as member stars as a consequence of the small difference between field and cluster proper motions.

The secondary main sequence and giant branch like structures completely vanished within the range of the proper motions. Below  $V = 14$  mag, we still find some stars remaining in the region of these features. Since the vector point plot diagram does not give any evidence for a second cluster in the same line of sight, we assume that these stars belong to the field star population(s). It is very unlikely, too, that the remaining stars are pre main sequence cluster members, because at the age of NGC 581 (see the following paragraph) this kind of objects should be much closer to the main sequence than the stars in the CMD are (Iben 1965). Therefore we assume these stars to be remnants of the field star subtraction due to the imperfect statistics of the sample.

**Table 8.** Parameters of NGC 581 as derived from isochrone fitting to the colour magnitude diagram. The errors of distance modulus and reddening are estimated, the uncertainty of the age is derived from the comparison with the isochrones neighbouring the selected one

distance modulus	$(m - M)_0 = 12.3 \pm 0.1$ mag
i.e. distance	$r = 2884 \pm 130$ pc
reddening	$E_{B-V} = 0.41 \pm 0.02$ mag
age	$\log t = 7.2 \pm 0.1$
i.e.	$t = 16 \pm 4$ Myr
metallicity	$Z = 0.02$

We fitted isochrones of the Geneva group (Schaller et al. 1992) to the resulting CMD from which we derived the distance modulus, reddening, age, and metallicity of NGC 581. The best fitting isochrone is plotted into the cleaned CMD of Fig. 8. The parameters of the selected isochrone are shown in Table 8. Isochrones of the Padua group (Bertelli et al. 1994) were fitted to the CMD for comparison and led to the same set of parameters.

#### 4.3. Completeness correction

To obtain comprehensive luminosity and initial mass functions, the data have to be corrected for completeness. As crowding is not a problem in our images, the completeness in the field and cluster regions are the same so that it is not necessary to correct for completeness before the field star subtraction.

With artificial star experiments using the DAOPHOT II routine `addstar` we derived the completeness function shown in Fig. 9. As the  $V$  images reach down to much fainter magnitudes, these experiments were only performed with the  $B$  exposures. Down to  $B = 17.25$  mag the sample is more than 80% complete with a sharp drop afterwards to almost 0% at  $B = 19$  mag. Fig. 9 shows that the completeness level of 60% is reached around  $B = 18$  mag, so that we assume this value to be a reasonable cut-off for our studies. With a main sequence star colour of  $B - V = 0.8$  mag for  $B = 18$  mag, this corresponds to a limiting magnitude of  $V = 17.2$  mag.

#### 4.4. Initial mass function

With the stars of the cleaned CMD we determined the luminosity (Fig. 10) and initial mass functions of NGC 581 after deleting all objects outside a  $\Delta(B - V) = 0.3$  mag wide strip around the main sequence and above the turnover of the isochrone around  $V = 10$  mag from the CMD and applying the completeness correction described in Sect. 4.3. As mentioned in Sect. 3.2, some field stars will have stayed in the sample while a few cluster stars might have been rejected. However, we assume these two effects do not influence the IMF of NGC 581.

From the initial stellar masses given in the Geneva isochrone data, we computed a mass-luminosity relation represented by a 6<sup>th</sup> order polynomial:

$$m[M_{\odot}] = \sum_{i=0}^6 d_i \cdot V^i [\text{mag}] \quad (7)$$

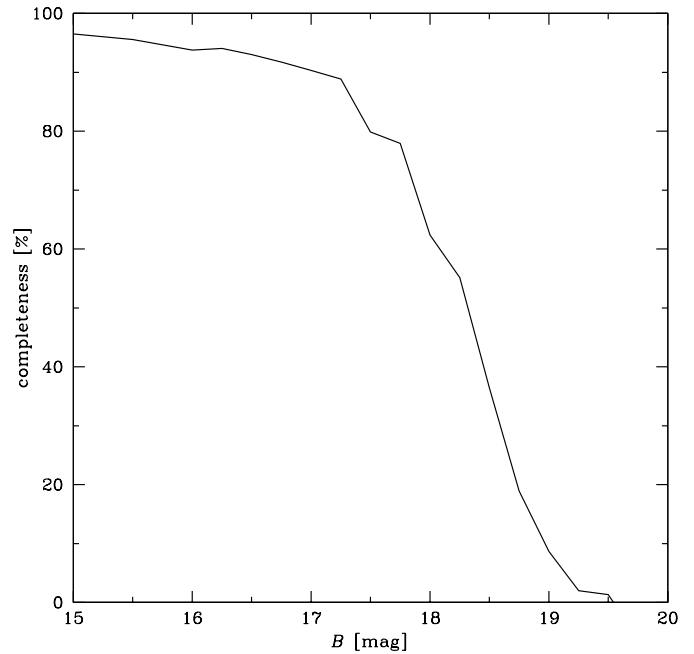


**Fig. 9.** Diagram of the completeness of our data as a function of  $B$  magnitudes. Down to  $B = 17.25$  mag, the sample is more than 90% complete, down to one magnitude fainter, we detect a completeness of more than 50%. After this point, the completeness sharply drops until no more stars are being detected at  $B = 19.5$  mag. For our further investigations we skip all stars fainter than  $B = 18$  mag which corresponds to a completeness level of higher than 60%

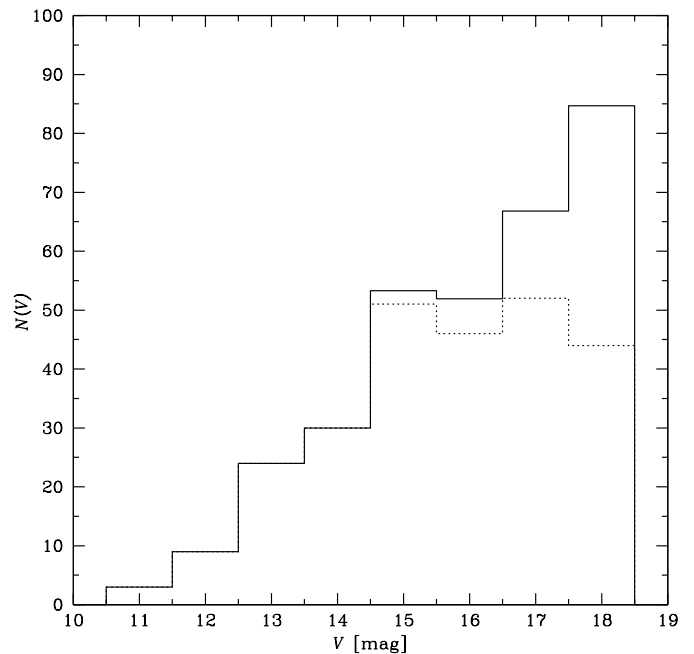


**Fig. 10.** Luminosity function of NGC 581. The histogram obtained after completeness correction is printed with solid, the uncorrected one with dotted lines

with the following parameters:

$$d_0 = -523.815$$

$$\begin{aligned}
 d_1 &= +221.123 \\
 d_2 &= -36.347 \\
 d_3 &= +3.055 \\
 d_4 &= -0.140 \\
 d_5 &= +0.003 \\
 d_6 &= -0.0000327.
 \end{aligned}$$

A 5<sup>th</sup> order polynomial still did not fit the faint part of the mass-luminosity relation well enough. With Eq. (7) we derived the initial masses of the stars classified as objects of NGC 581 on the base of their  $V$  magnitudes.  $V$  was preferred compared with the  $B$  values as their photometric errors are smaller at equal magnitudes.

We included all stars with a mass of higher than  $m = 1.41M_{\odot}$  (corresponding to the previously mentioned value of  $V = 17.2$  mag or  $\log m = 0.15$ ). In this range, the completeness is 60% or higher. 198 stars were selected by this criterion. The stars were divided in  $\Delta \log m = 0.1$  wide bins. The star numbers were corrected using the results of the completeness calculation, resulting in 247 “virtual” stars from  $9.45M_{\odot}$  down to  $1.41M_{\odot}$ . The resulting histogram is presented in Fig. 11. The single star with a mass around  $9.45M_{\odot}$  ( $\log m = 0.98$ ) was not taken into account for the IMF determination, since this single object at one end of the histogram might heavily influence the IMF slope. The slope of the IMF was determined by linear regression to the histogram.

We obtained  $\Gamma = -1.80 \pm 0.19$  from the stars with a mass from  $1.41M_{\odot}$  to  $8.70M_{\odot}$  (An experiment including the  $9.45M_{\odot}$  star led to  $\Gamma = -2.11 \pm 0.23$  and therefore to a difference in the exponent of more than 0.3!). The resulting IMF is shown in Fig. 11.

## 5. Summary and discussion

NGC 581 is a young open star cluster with an age of 16 Myr. It is located at a distance of 2900 pc from the Sun. We derived proper motions of 228 stars in the region of the cluster down to 14 mag. 77 of those can be considered members of the object. A study of the IMF of NGC 581 leads to a power law with a slope of  $\Gamma = -1.80$ .

The results of the photometry mainly coincide with the findings of Phelps & Janes (1993), however, we do not find evidence for a star formation over a period of as long as 10 Myr: While Phelps & Janes claim the necessity of two isochrones of different ages to fit both the blue and red bright stars in their CMD, the Geneva  $\log t = 7.2$  isochrone fits all features of our CMD sufficiently well.

The IMF slope might be slightly higher than Scalo’s (1998) figure for this mass range, as Phelps & Janes (1994) find a steep slope for NGC 581, too. Their value of  $\Gamma = -1.78$  marks the steepest IMF of their entire study of open star clusters. Although their IMF is based on a photometry with a deeper limiting magnitude, our determination has its advantages, too: Phelps & Janes only used statistical field star subtraction and no information of proper motions, which may have great impact on the high mass

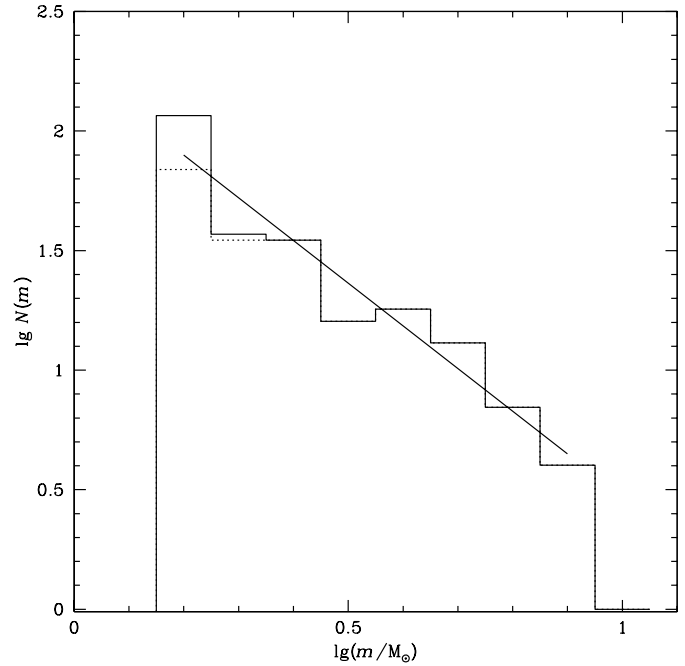


**Fig. 11.** Initial mass function of NGC 581. The solid line corresponds to the completeness corrected values, the dotted line to the original data. The IMF slope calculated with linear regression to the histogram is determined to be  $\Gamma = -1.80 \pm 0.19$

range and therefore might affect the slope of the IMF. Furthermore, they only took one single region in the vicinity of their star clusters for the field star subtraction, while we were able to use the surrounding of the cluster itself. And finally, their field of view is so small that they probably did not cover the entire cluster which, assuming the presence of mass segregation, might have flattened their IMF due to a lack of low mass stars from the outer regions of the cluster.

If we would not have based part of the membership determination on the proper motions, we would have ended up with 9 more stars in the magnitude range of  $V < 14$  mag (see Fig. 7). Since the total star number in this region is low, this would have decreased the IMF the slope to  $\Gamma = 1.73 \pm 0.28$ . Within the errors, this result would still match with our value above, however, the shape of this IMF is less well represented by a power law, which is expressed by the higher error. Therefore we claim that adding the information of the field star subtraction did improve the reliability of our IMF study.

*Acknowledgements.* The authors acknowledge Wilhelm Seggewiss for allocating time at Hoher List Observatory and Albert Bruch for time at the Münster PDS machines. Thanks a lot to Andrea Dieball for the field star subtraction software and to Klaas S. de Boer and Andrea Dieball for carefully reading the manuscript of this publication. J.Sa. especially thanks Thomas Schimpke for introducing him to the use of PDS and the software for handling the digitised photographic plates and Georg Drenkhahn for his support in programming IRAF scripts. J.B. acknowledges financial support from the Deutsche Forschungsgemeinschaft under grant ME 1350/3-2.

**References**

- Bertelli G., Bressan A., Chiosi C., Fagotto F., Nasi E., 1994, *A&AS* 106, 275
- Brunzendorf J., Meusinger H., 1998, in: Brosche P., Dick W.R., Schwarz O., et al. (eds.) *The Message of the Angles – Astronomy from 1798 to 1998*, 148
- Dieball A., Grebel E., 1998, *A&A* 339, 773
- ESA, 1997, *The HIPPARCOS and Tycho Catalogues*. ESA SP-1200
- Francis S.P., 1989, *AJ* 98, 888
- Geffert M., Klemola A.R., Hiesgen M., Schmolz J., 1997, *A&AS* 124, 157
- Hoag A.A., Johnson H.L., Iriarte B., et al., 1961, *Pub. US Naval Obs.* 17, 347
- Iben I., 1965, *ApJ* 141, 993
- Phelps R.L., Janes K.A., 1993, *AJ* 106, 1870
- Phelps R.L., Janes K.A., 1994, *ApJS* 90, 31
- Purgathofer A., 1964, *Ann. Wien* 26, 37
- Salpeter E.E., 1955, *ApJ* 121, 161
- Sanders W.L., 1971, *A&A* 15, 173
- Sanner J., Dieball A., Schmolz J., Reif K., Geffert M., 1998, in: Lopez Garcia A., Yagudin L.I., Martínez Usó M.J., et al. (eds.) *IV International Workshop on Positional Astronomy and Celestial Mechanics 1996*, 373
- Scalo J.M., 1986, *Fund. Cosm. Phys.* 11, 1
- Scalo J.M., 1998, *ASP Conf. Series* 142, 201
- Schaller G., Schaerer D., Meynet G., Maeder A., 1992, *A&AS* 96, 269
- Stetson P.B., 1991, In: Grosbøl P.J., Warmels R.H. (eds.) *38<sup>th</sup> ESO/ST-ECF Garching Data Analysis Workshop*, 187
- Subramaniam A., Gorti U., Sagar R., Bhatt H.C., 1995, *A&A* 302, 86
- Tsujimoto T., Yoshii Y., Nomoto K., et al., 1997, *ApJ* 483, 228
- Wielen R., Dettbarn C., Jahreiß H., Lenhardt H., Schwan H., 1999, *A&A* 346, 675